

Vibration response imaging in idiopathic pulmonary fibrosis: a pilot study

Qing-xia Liu^{1*}, M. Med.; Wei-jie Guan^{2*}, Ph. D.; Yan-qing Xie², Ph. D.; Jia-ying An², M. B.; Mei Jiang^{2*}, Ph. D.; Zheng Zhu², M. Med.; E Guo², M. Med.; Xin-xin Yu², M. B.; Wen-ting Liu², M. B.; Yi Gao², M. Med.; Jin-ping Zheng², M. D.

¹ Qingyuan People's Hospital, Qingyuan, Guangdong 511518, China

² State Key Laboratory of Respiratory Disease, First Affiliated Hospital of Guangzhou Medical University, Guangzhou, Guangdong 510120, China

Correspondence: Jin-ping Zheng, M. D., State Key Laboratory of Respiratory Disease, First Affiliated Hospital of Guangzhou Medical University. Address: 151 Yanjiang Road, Guangzhou, Guangdong, China. Fax: +86-20-83062729, Tel: +86-20-83062869, E-mail: jpzhenggy@163.com.

***Qing-xia Liu and Wei-jie Guan shared first co-authorship.**

Conflict of interest: None declared.

Abbreviations: CT= computed tomography; DLCO-SB% pred= diffusing capacity of carbon monoxide per predicted measured by single-breath method; EVP= envelope of acoustic signal; FVC= forced vital capacity; FVC%pred= forced vital capacity predicted; FEV₁= forced expiratory volume in one second; FEV₁%pred= forced expiratory volume in one second predicted; IPF= idiopathic pulmonary fibrosis; MEF= maximal energy frame; QLD= quality lung data; VRI= vibration response imaging

Abstract

Background: Although vibration response imaging (VRI) is a novel imaging technique, little is known about its characteristics and diagnostic value in idiopathic pulmonary fibrosis (IPF).

Objective: To investigate the features of VRI in IPF subjects.

Methods: We enrolled 23 subjects with IPF (42-74 years) and 28 healthy subjects (42-72 years). Subjects with IPF were diagnosed by lung biopsy, and underwent VRI, spirometry, lung diffusing test, chest X-ray or computed tomography, which entailed assessment of the value of VRI indices.

Results: The VRI total score correlated statistically with $D_LCO-SB\%pred$ ($r_s = -0.30$, $P = .04$), but not with $FVC\%pred$, $FEV_1\%pred$ and FEV_1/FVC ($r_s = -0.27, -0.22$ and 0.19 , all $P > .05$). Compared with healthy subjects (17.9%), 20 subjects with IPF (86.96%, $P < .01$) presented with significantly increased crackles. The difference in QLD in all lung regions was unremarkable (all $P > .05$), except for the upper right and lower left lobe ($P < 0.05$). Overall, VRI parameters yielded acceptable assay sensitivity and specificity. MEF was characterized by the highest diagnostic value (sensitivity: 1.000, specificity: 0.824), followed by presence of enormous crackles (sensitivity: 0.696, specificity: 0.964). VRI total score was not a sensitive indicator of IPF owing to low assay sensitivity (0.696) and specificity (0.643).

Conclusion: VRI technique may be helpful to discriminate IPF subjects from healthy individuals. MEF and abundant crackles might serve as a diagnostic tool of IPF.

Key words: idiopathic pulmonary fibrosis; pulmonary function, pulmonary breathing imaging diagnosis system; vibration response imaging

Short title: Vibration response imaging in IPF

Abstract count: 220 words

Text count: 2295 words

Introduction

Idiopathic pulmonary fibrosis (IPF), characterized by dyspnea on exertion, hypoxia, restrictive ventilatory dysfunction, reduced diffusing capacity and pulmonary fibrosis on chest computed tomography (CT), has been increasingly recognized as a diversity of disorders involving the pulmonary interstitium and (or) parenchyma. The gold standard of diagnosis of IPF relies on lung biopsy, and the diagnosis can be achieved by chest imaging and lung function tests¹. In addition, the fact that measurement of diffusing capacity failed to identify the presence of IPF² suggested that conventional invasive measures might have limited significance. In this regard, the development of novel non-invasive technique with improved diagnostic power is urgently indicated.

Vibration response imaging (VRI) is a novel technique in which the diagnostic information is derived from the vibration energy superimposed on the respiratory cycles. The turbulent air and vibration generated within the airways could be sensitively captured by the sensors, thus allowing for a non-invasive, radiation-free and convenient approach to be clinically applied. VRI imaging system has been increasingly applied for the diagnosis of respiratory diseases, including chronic

obstructive pulmonary disease^{3,4}, asthma⁵, airway foreign body⁶, pleural effusion⁷ and pneumonia⁸. Furthermore, VRI plays a role in the assessment of lung function in regions of interest⁹, intervention treatment of pulmonary diseases¹¹, screening of candidates for lung surgery¹⁰, monitoring post-intubation conditions¹¹. Unfortunately, whether or not VRI has a high diagnostic power to IPF remains poorly studied. We hypothesized that subjects with IPF may have distinct characteristics as compared with healthy subjects and that the major VRI indices, as previous studies suggested, are useful to the diagnosis of IPF.

Consequently, we sought to determine the characteristics and diagnostic value of VRI imaging in subjects with IPF, thereby offering the rationale for clinical application.

Subjects and Methods

Subjects

We recruited 51 subjects, including 23 subjects with IPF (42-74 years) from the out-subject clinics and 28 healthy subjects (42-72 years) from Health Check-up Center of The First Affiliated Hospital of Guangzhou Medical University, between September 2011 and January 2012. The inclusion criteria comprised of: 1) subjects of either sexes with IPF¹²; 2) clinically diagnosed by typical chest CT pathologic characteristics of IPF; 3) absence of miscellaneous severe systemic diseases. Those with rib cage or spinal deformity or skin lesions or limited understanding were excluded.

Inclusion criteria for healthy subjects consisted of: (1) non-smokers of either sex; (2) normal chest radiograph; (3) normal spirometry and diffusing capacity; (4) absence of upper respiratory tract infection within 4 weeks; (5) no evidence of other chronic cardiopulmonary diseases. All

subjects gave written informed consent prior to the study. This study protocol was approved by the Ethics Committee of the First Affiliated Hospital of Guangzhou Medical University (No. 2012-26).

Study protocol

This was a single center study. All consecutive clinically stable subjects, characterized by no significant change (<20%) in the frequency of cough, sputum volume and spirometry and degree of dyspnea, underwent chest X-ray/CT, VRI imaging, spirometry and measurement of diffusing capacity, in this order. The date of biopsy differed from the out-subject visit and was typically 3 months apart. For healthy subjects, the need to perform chest X-ray was waived. These entailed subsequent analysis on the VRI indices.

Lung function testing

Spirometry (QUARK 4, COSMED Co. Ltd, Italy) and measurement of diffusing capacity using single-breath carbon monoxide wash-out method (QUARK 4, COSMED Co. Ltd, Italy) were conducted according to the 2005 guidelines by American Thoracic Society and European Respiratory Society^{13,14}.

Briefly, for spirometry, FVC, FEV₁, FVC%pred, FEV₁%pred and FEV₁/FVC were analyzed. At least 3 (not more than 8) maneuvers were performed, with the variation between the best two maneuvers of <5% or 150ml in FVC and FEV₁. The maximal values of FVC and FEV₁ were reported.

For single-breath carbon monoxide wash-out technique, the carbon monoxide diffusing capacity (D_LCO-SB) and the percentage predicted (D_LCO-SB%pred) were analyzed. The interval

between two consecutive measurements was not less than 4 min, and the variation coefficient for D_LCO-SB should be less than 10% or $3\text{ml}/(\text{min}\cdot\text{mmHg})$. The D_LCO-SB was reported based on the mean of the two measurements.

Brief overview of VRI

The VRI system (Deep Breeze Co. Ltd., Israel), by employing an array of specific sensors orderly placed on the pulmonary projection regions of the subject's back, is capable of capturing the changes in vibration as reflected by the constantly altered airflow (Figure 1). This entailed simulation of primitive mechanical signals that allowed transformation into digital signals for deriving the band-pass filtered images based on real-time sampling, thus reflecting dynamic variation in the breathing cycles. The major indices and their significance are introduced in the VRI image analysis section (See below and Online Supplement).

Critiques of VRI

VRI testing was performed in a quiet, noise-free chamber. Subjects were, following a 5-minute resting period, seated and placed with two sensor arrays on the back. These sensor arrays were placed bilaterally in parallel at the longitudinal and vertical axis (± 1.0 cm) and at least 2.5 cm away from the spine. The top-row sensors were positioned 1.5-2.0 cm superior to the shoulder blade. Subjects were instructed to breathe normally via the mouth during a 12-second recording (3 to 5 respiratory cycles). Forced exhalation or miscellaneous artifacts should be avoided. Subsequent tests were conducted at 1-to-2-minute intervals. This was followed by selection of a smooth vibration energy curve and maximal energy frame (MEF) image for further analysis. Tolerability of

test was assessed by inquiry of discomforts during the measurement.

VRI image analysis

VRI imaging analysis was conducted according to the vibration energy graph, dynamic image, maximal energy frame (MEF), quality lung data (QLD), envelope of acoustic signal (EVP) and presence of wheezes or crackles, whose definitions were showed in online supplement. The images of each individual were rated, for calculation of the total score, based on of the features as outlined in e-Table 1 (Online supplement). The normal VRI images are shown Figure 2.

Statistical Analysis

Data were analyzed using SPSS version 16.0 for Windows (SPSS Co. Ltd, Chicago, IL). Continuously distributed variables were presented as mean \pm standard deviation following test of normality. Student's t test or χ^2 test was used to compare the difference between both groups, depending on the distribution pattern of variables. Spearman Correlation analysis was applied to analyze the correlation between VRI and spirometric parameters and diffusing capacity. The diagnostic performance of VRI total score, MEF and presence of crackles was compared. $P < 0.05$ was defined as statistically significant.

Results

Baseline demographic characteristics

Subjects with IPF did not differ statistically with healthy subjects in terms of age ($P = .82$) and height ($P = .18$). The difference in weight and male-to-female ratio were statistically (both $P < 0.05$)

but not clinically significant. Lung function parameters, including FVC ($t=3.52$, $P < .01$), FVC%pred ($t=9.02$, $P < .01$), FEV₁%pred ($t=-5.32$, $P < .01$) and D_LCO-SB%pred ($t=10.63$, $P < .01$) in IPF subjects were significantly lower than those in healthy subjects, with the exception of a higher FEV₁/FVC ($t=-3.59$, $P < .01$, Table 1).

Dynamic image

The VRI total score correlated statistically with D_LCO-SB%pred (Figure 3, $r_s = -0.30$, $P = 0.04$), but not with FVC%pred ($r_s = -0.27$, $P = 0.06$), FEV₁%pred ($r_s = -0.22$, $P = 0.13$) and FEV₁/FVC ($r_s = 0.19$, $P = 0.19$).

Features of MEF image

The MEF image of healthy subjects evidenced a comparatively even distribution of the vibration energy, as reflected by the gradient of grey-scales. The grossly symmetric pattern of the vibration energy could be noted bilaterally. (Figure 4-A) In contrast, subjects with IPF demonstrated a totally different pattern from healthy subjects. This included bilaterally constrained regions of vibration energy, triangle-like distribution of maximal energy that was restricted to and intensified in the lower lobes, and weakened intensity of vibration energy in the upper lobes (Figure 4-B). Such features were not found in miscellaneous respiratory diseases, i.e. asthma and COPD (data not shown).

EVP image

Subjects with IPF, similar with healthy subjects, demonstrated a slight inconsistency between

EVP signals in the right and left lung (Figure 5).

Adventitious Lung Sounds

20 subjects with IPF (20/23, 86.96%) presented with significantly increased crackles (blue dots in Figure 6-A) compared with that of healthy subjects, of whom 5 (5/28, 17.9%, $P < .01$) presented with minor crackles (Figure 6-B).

Quality lung data

The difference in QLD in all lung regions was unremarkable (all $P > .05$), except for the upper right and lower left lobe ($P = .01$). (Table 2)

Diagnostic power of major VRI indices

Overall, VRI parameters yielded acceptable assay sensitivity and specificity. MEF was characterized by the highest diagnostic value, followed by presence of enormous crackles. The VRI total score did not appear to be a sensitive marker indicative of IPF. The diagnostic indices of EVP and QLD could not be derived and was therefore not analyzed in the current study. (Table 3)

Discussion

Our data showed that, compared with vibration energy images in healthy subjects (Figure 2), IPF subjects were characterized by bilaterally constrained vibration energy, triangle-like distribution of maximal energy that was restricted to and intensified in the lower lobes, and

weakened intensity of vibration energy in the upper lobes. There was a positive correlation between the VRI total score and $D_LCO-SB\%pred$. IPF subjects also had an increased number of crackles as the adventitious lung sounds compared with healthy subjects. MEF and presence of enormous crackles were the VRI indices with highest diagnostic power.

IPF is a diversity of diseases characterized by various clinical and imaging features. Typically, restrictive ventilatory dysfunction (reduced FVC and FEV_1 yet normal FEV_1/FVC) and reduced diffusing capacity (low D_LCO-SB) may be readily identified in most subjects, particularly those with increased disease severity. Although there have been limited literatures regarding the detailed interpretation of changes observed in VRI indices, it is likely that the highly restricted vibration energy shown in MEF images could have stemmed from restrictive ventilatory dysfunction. The upper lung lobes may theoretically have a priority for ventilation, which appeared inconsistent with our finding that less vibration energy was focused.

Another major finding of the current study was that the VRI total score correlated positively with $D_LCO-SB\%pred$, a parameter reflecting the diffusing capacity, suggesting that subjects with poorer diffusing capacity were more likely to have aberrant VRI grading. Unfortunately, the fact that the total grade of VRI was correlated with neither $FVCpred\%$ nor $FEV_1pred\%$ has rendered it tough to interpret the results inasmuch that these two indices clinically remained the major approaches for determining, at least physiologically, the severity of IPF.

The significance of VRI total score has been compelling. Previous reports documented that subjects with pneumonia⁸ and COPD⁴ had a markedly higher total score than healthy individuals (e-Table 2), suggesting that an increased total score might be an insensitive marker of pulmonary diseases. However, higher scores indicating more significant anomaly were negatively correlated

with DLCO-SB%pred. Whether or not the VRI total score may help predict the severity of IPF necessitates further studies in a larger population.

Despite that IPF subjects had slightly lower maximal vibration energy than the healthy subjects, the difference between the two groups appeared statistically insignificant, possibly because of an insufficient number of subjects enrolled in the study. It is also likely that the maximal vibration energy has a limited diagnostic power to IPF.

QLD data did not seem to be an appropriate diagnostic tool for IPF. This was in line with the fact that, in subjects with IPF, QLD failed to increase in bilateral lower lobes. The value of QLD data remain to be further investigated in successive studies.

Of 23 subjects with IPF who had typical changes of MEF images in the present study, 6 did not exhibit evidence of restrictive ventilatory dysfunction. This has led us to speculate that aberrant VRI indices might precede lung function decline, rendering it a more sensitive technique for IPF. MEF might be a candidate for the diagnosis of IPF inasmuch that changes in MEF image were typically seen in subjects with IPF but not in healthy subjects. MEF images were deemed as a critical index for diagnosis of IPF, particularly when combined with miscellaneous parameters, including dynamic image, EVP or adventitious lung sounds. Furthermore, features of MEF image in IPF could be readily distinguished from COPD, asthma and other common respiratory diseases. (e-Table 2) This might be because of its capacity of displaying early-stage pulmonary physiological changes, which were considered as the consequence of poor living environments and air pollution. Importantly, none of the healthy subjects showed changes in MEF image typically witnessed in subjects with IPF. It was unlikely that the high sensitivity of MEF curve, but not the remaining VRI indices, was related to the sample size in our study.

Several major limitations must be considered. Firstly, our small sample size stemmed from the fact that IPF is a respiratory disease with a relatively low incidence compared with asthma and COPD. An increased sample size could render the distinct characters of IPF to be clearly displayed in different disease severity. However, our major findings remained robust as the typical VRI manifestations of IPF could be characterized and the parameter with high diagnostic performance was captured. Secondly, comparison on VRI features between subjects with IPF and other respiratory diseases such as COPD might advance our understanding regarding which VRI indices are more specific to reflect restrictive ventilatory dysfunction and poor diffusing capacity. Thirdly, it would be helpful if comparisons were made between subjects with interstitial pulmonary fibrosis and miscellaneous subtypes of IPF. Finally, the increased VRI total score, as mentioned previously, might not be specific to indicate presence of IPF, an investigation into more miscellaneous specific indices is necessary.

In summary, VRI technique may be helpful to discriminate IPF subjects from healthy individuals. MEF and an abundance of crackles might serve as a diagnostic tool of IPF. Further studies that investigate the features of VRI in IPF subjects with different disease severity and treatment response are indicated.

Acknowledgments

We would like to thank Ms. Bing-jie Kang and Deep Breeze Co. Ltd. (Israel) for providing the instrument and technical training.

Conflict of interest

All authors disclosed no financial support by any pharmaceutical company. The sponsor played no role in data analysis or interpretation of the results.

Author contributions

Qing-xia Liu, Wei-jie Guan conducted experiments, statistical analysis and drafted the manuscript.

Mei Jiang was responsible for confirming statistical method and part of the statistical analysis.

Jin-ping Zheng, Yan-qing Xie and Yi Gao steered study design and offered instructions.

Jin-ping Zheng took responsibility for revision and approval of submission of the manuscript.

Jia-ying An, Xin-xin Yu and Wen-ting Liu assisted in subject enrollment.

Reference

1. Grenier P, Brauner M. Imaging of fibrosing interstitial pneumonias. *Bull Acad Natl Med* 2010; 194 (2): 353-64.
2. Dunn TL, Watters LC, Hendrix C, Cherniack RM, Schwarz MI, King TE Jr. Gas exchange at a given degree of volume restriction is different in sarcoidosis and idiopathic pulmonary fibrosis. *Am J Med.* 1988; 85(2): 221-224.
3. Wang Z, Jean S, Bartter T. Lung sound analysis in the diagnosis of obstructive airway disease. *Respiration.* 2009; 77 (2):134–138.
4. Guntupalli KK, Reddy RM, Loutfi RH, Alapat PM, Bandi VD, Hanania NA. Evaluation of obstructive lung disease with vibration response imaging. *J Asthma.* 2008; 45(10): 923-30.
5. Waseem M, Reynolds T, Jara F, Gat Merav, Rozen D, Pollack C. Vibration response imaging breathing profile in acute asthmatic subjects before and after treatment (abstract). *Chest.* 2011: 140: 219A.
6. Dellinger RP, Parrillo JE, Kushnir A, Rossi M, Kushnir I. Dynamic visualization of lung sounds with a vibration response device: a case series. *Respiration.* 2008; 75 (1): 60-72.
7. Mor R, Kushnir I, Meyer J, Ekstein J, Ben-Dov I. Breath sound distribution images of subjects with pneumonia and pleural effusion. *Respir Care.* 2007; 52 (12): 1753-1760.
8. Bartziokas K, Daenas C, Preau S, Zygoulis P, Triantaris A, Kerenidi T, et al. Vibration Response Imaging: evaluation of rater agreement in healthy subjects and subjects with pneumonia. *BMC Med Imaging.* 2010; 10 (1): 6.
9. Becker HD, Slawik M, Miyazawa T, Gat M. Vibration response imaging as a new tool for interventional-bronchoscopy outcome assessment: a prospective pilot study. *Respiration.* 2009; 77

(2): 179-94.

10. Comce F, Bingol Z, Kiyan E, Tanju S, Toker A, Cagatay P, et al. Vibration-response imaging versus quantitative perfusion scintigraphy in the selection of subjects for lung-resection surgery. *Respir Care*. 2011; 56 (12): 1936-41.

11. Cinel I, Jean S, Tay C, Deal E, Parrillo JE, Dellinger RP. Case report: vibration response imaging findings following inadvertent esophageal intubation. *Can J Anaesth*. 2008; 55 (3): 172-6.

12. American Thoracic Society/European Respiratory Society. International multidisciplinary consensus classification of the idiopathic interstitial pneumonias. *Am J Respir Crit Care Med*. 2002; 19 (5): 794–796.

13. Miller MR, Hankinson J, Brusasco V, Burgos F, Casaburi R, Coates A, et al. Standardisation of spirometry. *Eur Respir J*. 2005, 26 (2):319-338.

14. MacIntyre NR, Crapo RO, Viegi G, Johnson DC, van der Grinten CP, Brusasco V, et al. Standardisation of the single-breath determination of carbon monoxide uptake in the lung. *Eur Respir J*. 2005; 26 (4): 720-735.

Figure legends

Fig 1--Schematic diagram of vibration response imaging

Fig 2-- Schematic diagram of normal VRI images. Panel A: MEF image showing typical distribution of vibration energy as reflected by the grey-scale; **Panel B:** QLD image showing distribution of vibration energy at different pulmonary fields; **Panel C:** Dynamic image showing synchronized vibrations without evidence of bouncing; **Panel D:** Vibration energy graph showing similar individual breathing cycle; **Panel E:** EVP image showing synchronized vibrations with equal amplitude.

Fig 3--Correlation between $D_lCO-SB\%pred$ and the VRI total score

Fig 4—Maximal energy frame (MEF) image. Panel A: MEF of a female healthy subject; **Panel B:** MEF of a female IPF subject

Fig 5—Envelope of acoustic signal curve in a female IPF subject

Fig 6--Adventitious lung sound. Panel A showing enormous crackles (blue dots) in a female IPF subject; **Panel B** showing minor crackles (blue dots) in a female healthy subject.

Table 1 Baseline Characteristics

Characteristic	Healthy subjects (n=28)	IPF subjects (n=23)	Statistics	P Value
Age (yrs)	55.86±1.71	56.43±1.86	-0.23	.82
Height (cm)	157.5±1.47	160.52±1.61	-0.14	.18
Weight (kg)	58.05±1.89	65.94±1.63	-3.09	< .01
Male/female ratio (No.)	7/21	13/10	-2.27*	.02
FVC (L)	2.82±0.12	2.16±1.53	3.52	< .01
FVC%pred	103.68±2.15	68.45±3.43	9.02	< .01
FEV ₁ (L)	2.20±0.11	1.86±0.13	0.05	.34
FEV ₁ %pred	99.69±1.88	71.81±3.54	-5.32	< .01
FEV ₁ /FVC	80.43±1.20	86.10±0.95	-3.59	< .01
D _L CO-SB% pred	88.81±2.18	44.68±3.74	10.63	< .01
Total score	15.57±0.55	17.17±0.49	-2.15	.03
Maximum vibration energy	1,91±0.07	1.72±0.06	1.93	.06

*: for chi-square test; Student's t-test was applied for all other comparisons unless otherwise stated.

Table 2 Comparison on QLD in both groups

Lung region	Healthy group (n=28)	IPF group (n=23)	t value	P value
Upper right (%)	8.25±0.99	12.09±1.09	-2.59	.01
Middle right (%)	17.57±0.59	17.78±0.92	-0.20	.84
Lower right (%)	19.96±1.77	19.70±1.69	-0.11	.91
Total right (%)	45.79±1.98	49.57±1.88	-1.26	.18
Upper left (%)	12.36±0.62	13.96±1.03	-1.39	.17
Middle left (%)	19.89±0.98	19.87±1.19	0.41	.68
Lower left (%)	21.36±1.08	17.04±1.18	2.69	.01
Total left (%)	54.21±1.98	50.70±1.89	1.27	.21

Table 3 Diagnostic power of major VRI indices

Parameter	Sensitivity	Specificity	Youden's index	Positive likelihood ratio	Negative likelihood ratio
Total score	0.696	0.643	0.339	0.783	0.536
MEF	1.000	0.824	0.824	0.739	1.000
enormous crackles	0.696	0.964	0.660	0.870	0.821

MEF: maximal energy frame



Fig 1--Schematic diagram of vibration response imaging
69x94mm (300 x 300 DPI)

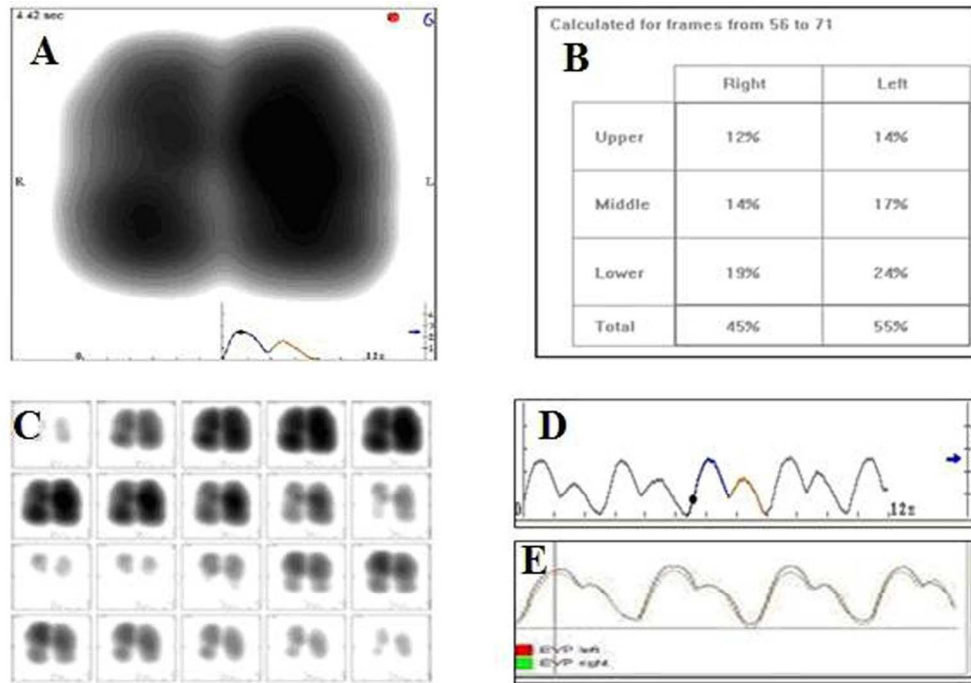


Fig 2-- Schematic diagram of normal VRI images. Panel A: MEF image showing typical distribution of vibration energy as reflected by the grey-scale; Panel B: QLD image showing distribution of vibration energy at different pulmonary fields; Panel C: Dynamic image showing synchronized vibrations without evidence of bouncing; Panel D: Vibration energy graph showing similar individual breathing cycle; Panel E: EVP image showing synchronized vibrations with equal amplitude.
152x104mm (300 x 300 DPI)

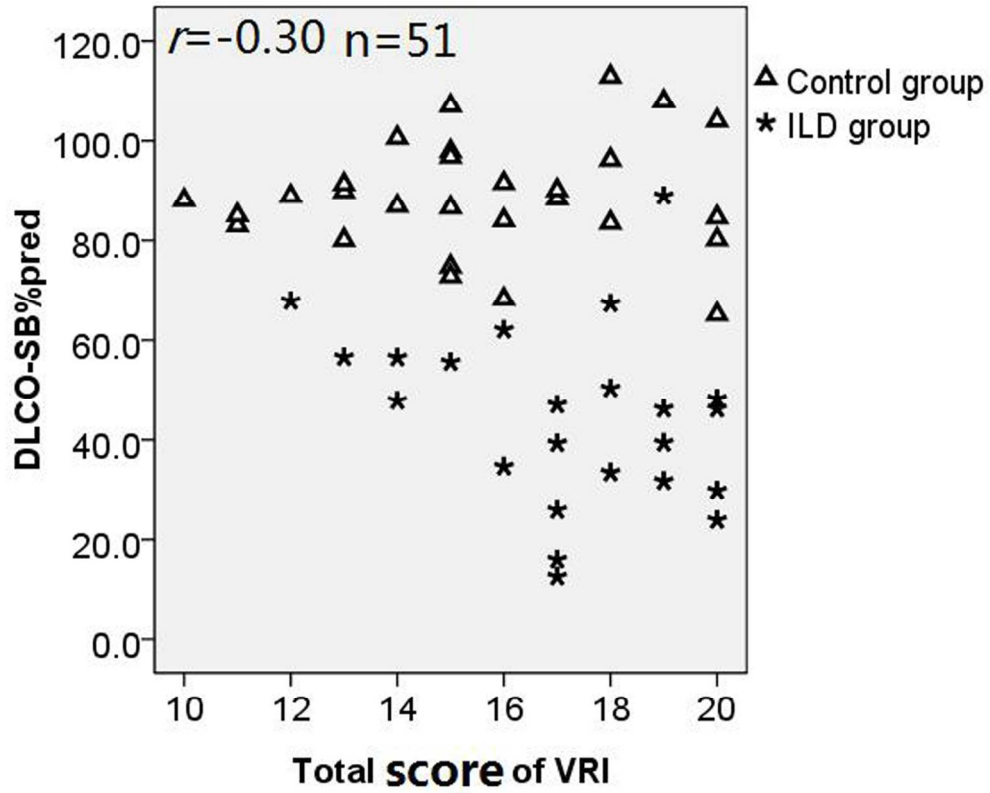


Fig 3--Correlation between DLCO-SB%pred and the VRI total score
159x126mm (300 x 300 DPI)

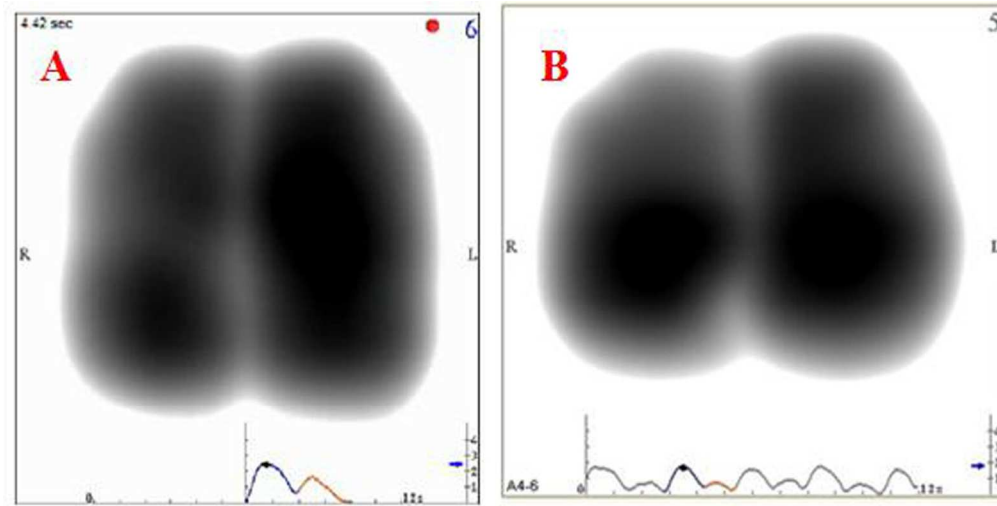


Fig 4—Maximal energy frame (MEF) image. Panel A: MEF of a female healthy subject; Panel B: MEF of a female ILD patient
150x75mm (300 x 300 DPI)

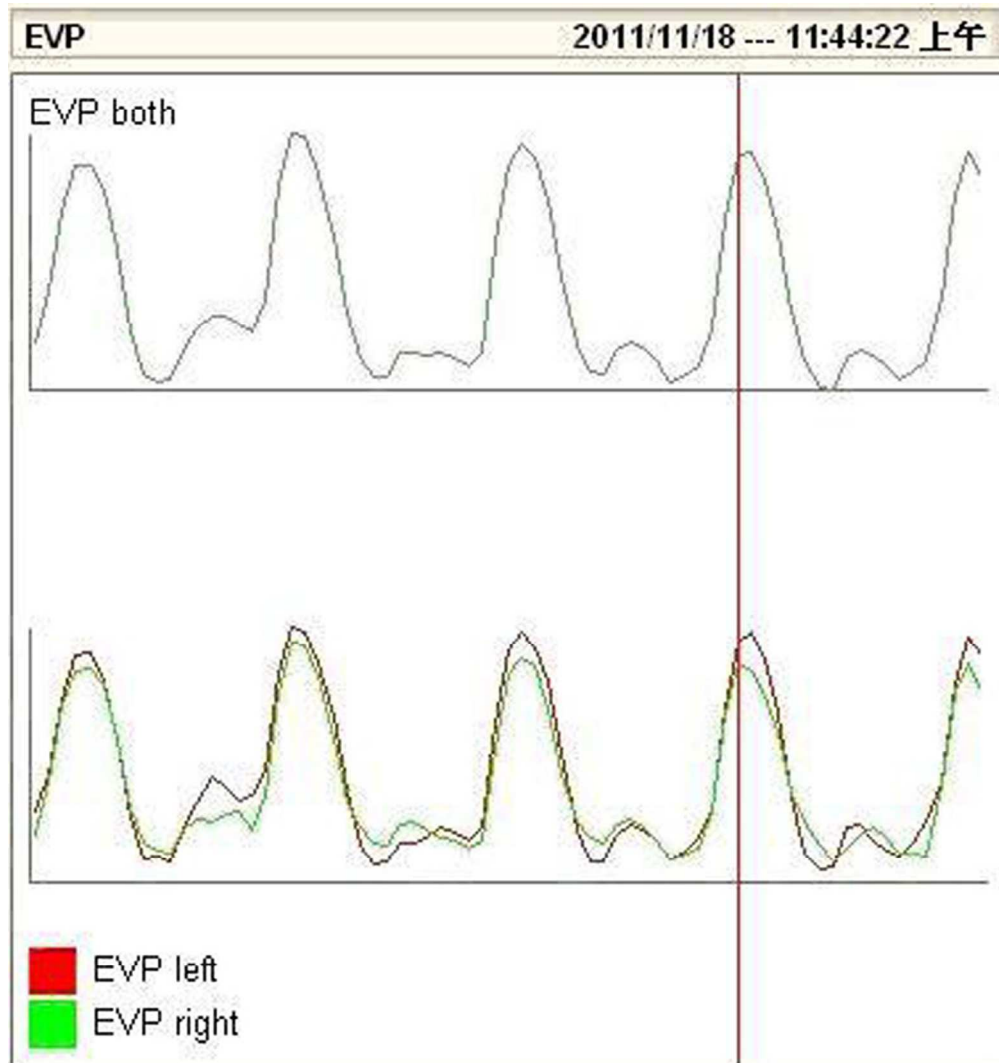


Fig 5—Envelope of acoustic signal curve in a female ILD patient
100x107mm (300 x 300 DPI)

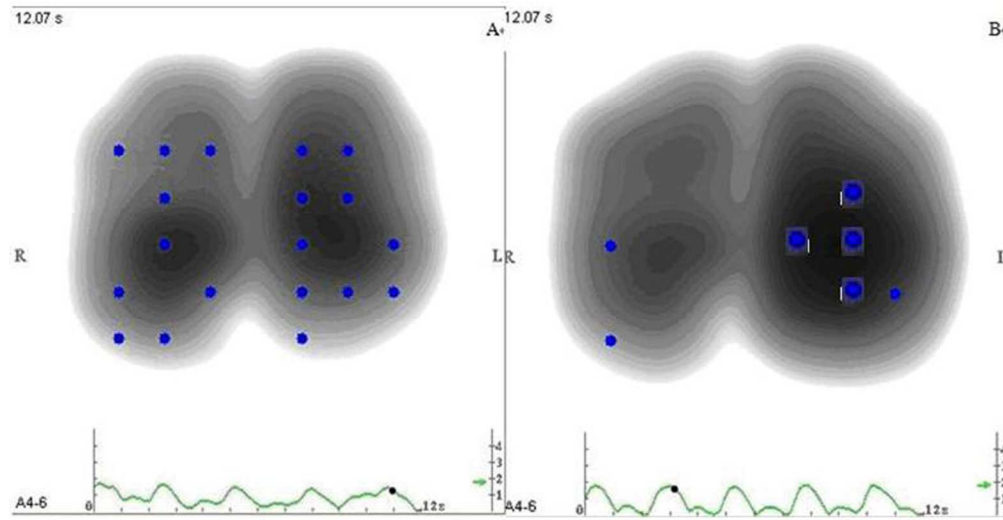


Fig 6--Adventitious lung sound. Panel A showing enormous crackles (blue dots) in a female ILD patient; Panel B showing minor crackles (blue dots) in a female healthy subject.
202x107mm (300 x 300 DPI)